Clays and Clay Minerals, Vol. 61, No. 4, 328–341, 2013.

COMBINED SALT AND TEMPERATURE IMPACT ON MONTMORILLONITE HYDRATION

PER DANIEL SVENSSON[1] AND STAFFAN HANSEN[2]

[1] Swedish Nuclear Fuel and Waste Management Co, Oskarshamn, Sweden
[2] Centre for Analysis and Synthesis, Department of Chemistry, Lund University, Sweden

Abstract—Bentonite is to be used as a sealing material for long-term storage of radioactive waste. During permafrost periods the buffer may freeze, causing the following: montmorillonite dehydration, ice formation, and pressure build-up that may fracture the surrounding rock. No previous study has been done on freezing of bentonite in saline water. Using small and wide angle X-ray scattering, the present study aimed to increase understanding of the combined impact of salt and temperature on the hydration (swelling) of Wyoming montmorillonite. The basal spacing of the Na-montmorillonite was very dependent on the water content, while this was not the case for the Ca-montmorillonite (after reaching 19 Å). The basal spacing of the free-swelling Na-montmorillonite (34−280 Å) was estimated successfully using simple calculations. During freezing of Na-montmorillonite in NaCl solution, both ice and hydrohalite formed (at −50 and −100ºC). At starting concentrations ⩾1.5 M the basal spacing was not affected by freezing. During freezing of Ca-montmorillonite in $CaCl_2$ solution, ice formed; antarcticite formed only sporadically. The basal spacing of the Ca-montmorillonite at high NaCl concentrations (>1 M) was greater at −50 and −100ºC (18 Å) than at 20ºC (16 Å). The opposite was observed at low concentrations. This change was attributed to small amounts of salts introduced into the montmorillonite interlayer, hence changing the interlayer water properties. The montmorillonite hydration was also temperature dependent; decreasing temperature increased the hydration (as long as no ice was formed) and increasing the temperature decreased the hydration. This was attributed to the temperature impact on the entropy of the hydration reaction. This observation was also reproduced in an experiment up to 90ºC. A small amount of salt in the groundwater was noted to reduce significantly the potential problem of ice formation in bentonite sealings.

Key Words—Äspö, Bentonite, Ca, Freezing, Hydration, Montmorillonite, MX-80, Na, Salt, SAXS, Sweden, Swelling, WAXS, XRD.

INTRODUCTION

The basal spacing of a Ca-montmorillonite with free access to liquid water is ~19 Å and in a simplified but useful and commonly used model this corresponds to a three water-layer hydrate, based on 3 Å per water layer and 10 Å for anhydrous montmorillonite (Bradley *et al.*, 1937). At sufficiently low temperature, the Ca-montmorillonite dehydrates during ice formation and hence the basal spacing decreases, at −50ºC to ~16 Å or a two water-layer hydrate (Svensson and Hansen, 2010). The same is noted for Na-montmorillonite with the major difference being that the basal distances may be even greater in liquid water. This freezing phenomenon of hydrated montmorillonite has been studied mainly by X-ray diffraction (XRD) (*e.g.* Norrish and Rausell-Colom, 1962; Ahlrichs and White, 1962; Anderson and Hoekstra, 1965; Low *et al*. 1968), but also by other techniques such as swelling-pressure measurements on confined and compacted specimens (Birgersson *et al*., 2008). The process is rapid and reversible, and the lower the temperature the more ice is formed on the outside of the montmorillonite which causes montmorillonite interlayer dehydration with smaller basal spacing (at least down to −50ºC; Svensson and Hansen, 2010). This is somewhat similar to the behavior of saline solutions. In liquid water at room temperature, NaCl and $CaCl_2$ occur as very hydrated ions, while at sufficiently low temperature ice forms together with the less hydrated phases hydrohalite ($NaCl{\cdot}2H_2O$; Light *et al*., 2009) and antarcticite ($CaCl_2{\cdot}6H_2O$; Torii and Ossaka, 1965). Although these systems (water-montmorillonite and water-salt) have been studied rather extensively on their own, the combined montmorillonite-water-salt system has received less attention. At low temperatures the authors have found no previous data on this combined system which has important technical applications, *e.g.* in a final repository of spent nuclear fuel, where freezing and thawing cycles of the bentonite buffer and backfill material must be considered (Birgersson *et al.*, 2008). The present study focuses on the combined impact of salt and temperature on the hydration of montmorillonite. The hydration was studied by synchrotron small- and wide-angle X-ray scattering (SAXS, WAXS). Because saline waters have lower freezing points, the temperatures −50 and −100ºC were chosen in order to compare the systems systematically (in the 3 M $CaCl_2$ case a kinetic experiment was also

* E-mail address of corresponding author:
daniel.svensson@skb.se
DOI: 10.1346/CCMN.2013.0610412

carried out down to −130ºC). The description of the number of layers of water in montmorillonite is a simplification but is justified by its practical value and is widely used in the literature. These layer-hydrates are labeled here as: W1 (one-layer hydrate), W2 (two-layer hydrate), W3 (three-layer hydrate), W4 (four-layer hydrate), and WX (unknown or indeterminable number of water layers). Listing the number of water layers in this way is a simplified concept of a more complex reality and a better description of the molecular structure of these water layers is found elsewhere (*e.g.* Tambach *et al.*, 2004). In the experiments, different mass fractions of montmorillonite in water were used. In this mass fraction the original hydrate water was not included (Ca-montmorillonite W2; Na-montmorillonite W1). Hence the total amount of water in the samples was slightly greater but this is accounted for in the calculations for predicting the basal spacings.

SAMPLES AND METHODS

Preparation of samples

The Na- and Ca-montmorillonite samples used in the present study were obtained courtesy of Clay Technology AB, Lund, Sweden. Homo-ionic and dialyzed clay fractions (<2 μm diameter) were prepared carefully from Wyoming-type bentonite (MX-80, American Colloid Co.). The analyses showed the clay fraction to consist almost exclusively of montmorillonite, with the following approximate layer composition per unit cell: $(Al_{3.1}Fe_{0.4}Mg_{0.5})(Si_{7.9}Al_{0.1})O_{20}(OH)_4$ and either Na- or Ca-ions in the interlayer positions (Karnland *et al*., 2006, p. 116). The bulk MX-80 used was milled in an agate mortar prior to use. The clays were not oven dried before use and hence contained some hydrate water (W1 for Na-montmorillonite; W2 for Ca-montmorillonite). The electrolytes used were 0−3 M NaCl and $CaCl_2$ (both pro analysi grade; Merck) along with natural groundwater from Äspö hard rock laboratory, Sweden. The Äspö water was sampled and analyzed by the chemical lab at Äspö Hard Rock Laboratory (SKB), Oskarshamn, Sweden. The water sample (SKB no 20069, bore hole KA 2858A) was filtered (Schleicher and Schuell 0.45 μm mixed cellulose ester filter) before analysis. Anions were determined using ion chromatography, except for chloride (titration) and fluoride (potentiometric analysis; Table 1). Major cations were analyzed by ALS Scandinavia, Luleå, Sweden, using inductively coupled plasma-atomic emission spectroscopy (Table 1). Ground montmorillonite was mixed with water or saline solution to form a paste with 30 wt.% of solid (or as otherwise specified). The samples with 70 and 80 wt.% montmorillonite were not really pastes and were more difficult to mix and to put into the capillaries. Some minor voids of air may have formed in these samples and in that sense were not fully water saturated. A capillary was partially filled with the paste and sealed with modeling clay (WAXS) or melt wax (SAXS). The samples used were thus essentially unoriented.

Small angle X-ray scattering (SAXS)

Data were collected at beamline I711 (Cerenius *et al*., 2000) at MAX-lab, Lund, using a Mar system with a flat CCD detector (Mar 165, 2048 × 2048 pixels). The X-ray beam had a wavelength of 1.099 Å. The wavelength was refined using a AgBEA standard (silver behenate; d_{001} = 58.4 Å; Huang *et al*. 1993), and the beam size was ~1 mm × 1 mm. The capillary was not rotated during the measurements. The sample–detector distance was 1643 mm and the air was evacuated from the system to avoid air scattering of the X-rays. The temperature during the SAXS measurements was constant at 20ºC. The maximum SAXS reflections were located visually; due to the complex background and low signal-to-noise ratio, no fitting routines were used. No corrections were applied to correct for the effect from the angular dependence of the scattering factors. The XRD patterns were presented in the figures with vertical offset and no background removal.

Wide angle X-ray scattering (WAXS)

Time-resolved or single-shot X-ray powder diffraction data were collected on beamline I711 as well as beamline I911-5 at MAX-lab (Mammen *et al*., 2002, 2004) using a Mar system with a flat CCD detector (Mar 165, 2048 × 2048 pixels). The X-ray beam had a wavelength of 1.099 Å, 0.994 Å (I711), 0.908 Å, or 0.954 Å (911-5) depending on the particular visit to the synchrotron. The wavelength was refined using a LaB_6 reference sample, and the beam size was ~1 mm × 1 mm. The capillary was not rotated during the measurements and was kept in a stream of flowing nitrogen with adjustable temperature (Cryojet, Oxford Instruments). The sample−detector distance used was 250−300 mm depending on the target 2θ range and resolution required

Table 1. Composition of a natural water sample from Äspö hard rock laboratory, Sweden (water section of the borehole (KA2858A) that was sampled between 39.77 and 40.77 m).

Concentration	Na	K	Ca	Mg	HCO_3	Cl	SO_4	Br	F	Si	Fe
mg/L	3420	12.8	4510	51.4	5.1	13500	624	107	1.33	5.17	<0.1
mM	149	0.33	112	2.12	0.08	381	6.50	1.34	0.07	0.18	<0.002

https://doi.org/10.1346/CCMN.2013.0610412 Published online by Cambridge University Press

(longer distance = greater resolution but smaller 2θ interval). After setting the target temperature, the data collection commenced. No continuous temperature monitoring was performed during the experiment. Each frame was monitored for ~20 s with subsequent saving of data until the final temperature was reached. Before and after each run, the absence of ice on the outside of the capillary was checked visually. The integrated intensity, scattering angle, and width of the recorded diffraction rings were evaluated using the *Fit2d* software (A.P. Hammersley, ESRF, pers. comm.: www.esrf.eu/computing/scientific/FJT2D/). The fitting was done by least-squares refining using Gaussian profiles and a linear background. The minimum scattering angle that was measured was ~1.7º2θ, depending on the exact position of the beam stop in each experiment. The XRD patterns were presented in the figures with vertical offset and without background removal unless otherwise stated.

RESULTS AND DISCUSSION

Na-montmorillonite at various solid-liquid ratios: SAXS at 20ºC

The greater the water content noted in the sample, the greater the basal spacing detected. At 80 wt.% clay in water, a basal spacing of ~19 Å was recorded, approaching the highest angle (smallest distance) detectable by the setup (Figure 1). At 70, 50, 30, and 10 wt.%, the 001 reflection was positioned at ~34 Å (0.7º2θ FWHM) and a weak peak at ~20 Å, 45 Å (0.8º2θ FWHM), 88 Å (1.1º2θ FWHM), and 280 Å, respectively. The given full width at half maximum (FWHM) is approximate. The identification of spacings at 280 Å probably approaches the limits of the method due to the low intensity of the reflection in relation to the background.

Na-montmorillonite in 0–1 M NaCl solution: SAXS at 20ºC

In pure water and 30 wt.% clay a basal reflection distance of ~88 Å was noted (Figure 2). In 0.25 M NaCl, a less pronounced reflection occurred at ~45 Å [~40 Å was observed by Norrish (1954) and 52 Å by Amorim *et al.* (2007) for 0.2 M]. At 0.5 M a simultaneous 20 and 40 Å spacing was observed by Norrish (1954), and a weak ~19 Å reflection with a further weak reflection at ~40 Å was observed in the present study, both reflections being very diffuse. At 1.0 M the 19 Å reflection increased in intensity and the lower-angle region of 1−2º looked steeper compared with that for 0.5 M. Norrish (1954) observed a 20 Å spacing at 1 M. A 17 Å reflection was observed at 0.5−1.0 M (Amorim

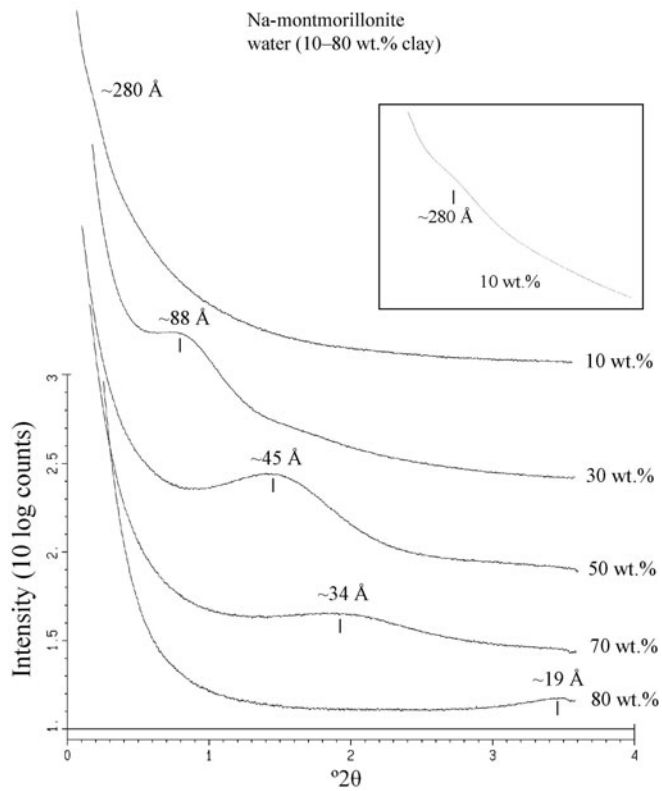

Figure 1. Small-angle X-ray scattering profiles of Na-montmorillonite at 10−80 wt.% clay in water. Inset: close up of the low-angle region of the 10 wt.% clay sample (λ = 1.099 Å).

https://doi.org/10.1346/CCMN.2013.0610412 Published online by Cambridge University Press

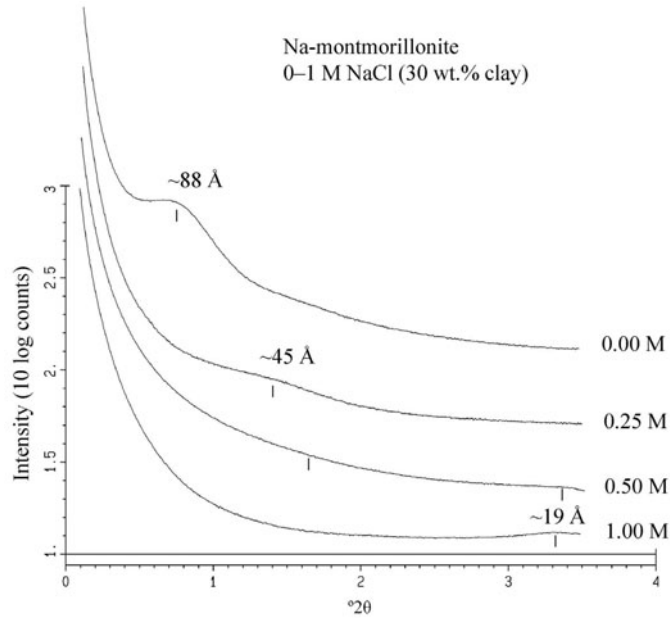

Figure 2. Small-angle X-ray scattering profiles of Na-montmorillonite at 0−1 M NaCl (30 wt.% clay; λ = 1.099 Å).

et al., 2007), which is a significantly lower *d* spacing. These observations (Figure 2) agreed with Norrish (1954) who found that salt concentrations (<1 M NaCl) had little or no effect on the crystalline swelling. The free swelling Na-montmorillonite (WX) was very sensitive to the saline content, however, and increasing saline concentration decreased the basal spacing of the free swelling phase linearly toward $1/\sqrt{C}$ (where C is the molar salt concentration). The salt increased the electrolyte concentration in the water (decreased the water potential) and this caused the dehydration of the montmorillonite by osmosis. The water potential is the potential energy of water relative to pure water in reference conditions, and it quantifies the tendency of water to move from one location to another due to osmosis, gravity, mechanical pressure, and matrix effects (*e.g.* surface tension and intermolecular forces). The transition between the three-layer hydrate W3 and the two-layer hydrate W2 took place at a relative humidity (RH) of ~95% in the case of Na-montmorillonite and at 90% for Ca-montmorillonite (Brindley and Brown, 1980: figures 3.3 and 3.4). Using Raoult's law and literature data on salt solutions (*CRC Handbook*, 1972), the W3 to W2 transition is calculated to take place at concentrations of 1.0 M NaCl and 1.8 M $CaCl_2$, respectively. A transition was observed in the experiments between 1.0 and 1.5 M in both cases (Figure 8) but is only an approximation as the salt that enters the montmorillonite interlayer is ignored.

Ca-montmorillonite in 0–1 M $CaCl_2$ solution: SAXS at 20ºC

In pure water, the basal spacing of the Ca-montmorillonite was determined to be 19.1 Å (W3) and was independent of the solid-liquid ratio (XRD traces not shown). Some tailing toward the low-angle side which decreased at greater electrolyte strength (0.1−0.5 M; Figure 3) was seen in pure water, which implies that a small proportion of the Ca-montmorillonite may swell beyond crystalline swelling similar to that seen in the Na-montmorillonite, *e.g.* tactoids of Ca-montmorillonite with internal 19 Å distances, with additional intertactoidial swelling. This has also been discussed previously by Svensson and Hansen (2010), based on *in situ* XRD measurement of Wyoming Ca-montmorillonite in deionized water during freezing and thawing cycles, and also by Segad *et al*. (2010), who performed dialysis experiments with Wyoming Ca-montmorillonite and referred to this additional swelling as "extra-lamellar swelling." At 1.0 M the basal spacing had decreased to 18.4 Å.

Na-montmorillonite in 0–3 M NaCl solution: WAXS at 20, –50, and –100ºC

At 20ºC, a gradual transition from a free-swelling montmorillonite (WX) to a two-water-layer montmorillonite occurred as the electrolyte strength increased in the samples from 0 to 3 M (Figure 4). At 0.25 M a mixture of WX and W3 was present, seen as a small distinct reflection overlapping the WX slope. At 1 M a W3 hydrate (19 Å) formed and above 1.5 M a W2 hydrate (15.8 Å). In all the −50 and −100ºC samples, W2 was present (15.8 Å). However, in 0.5 M and especially 1 M, W3 was also present, with an unresolved 001 peak at 17.8 Å. Hence, at intermediate electrolyte starting strength (~1 M), the basal spacing had a maximum among the low-temperature measurements (−50 and −100ºC).

https://doi.org/10.1346/CCMN.2013.0610412 Published online by Cambridge University Press

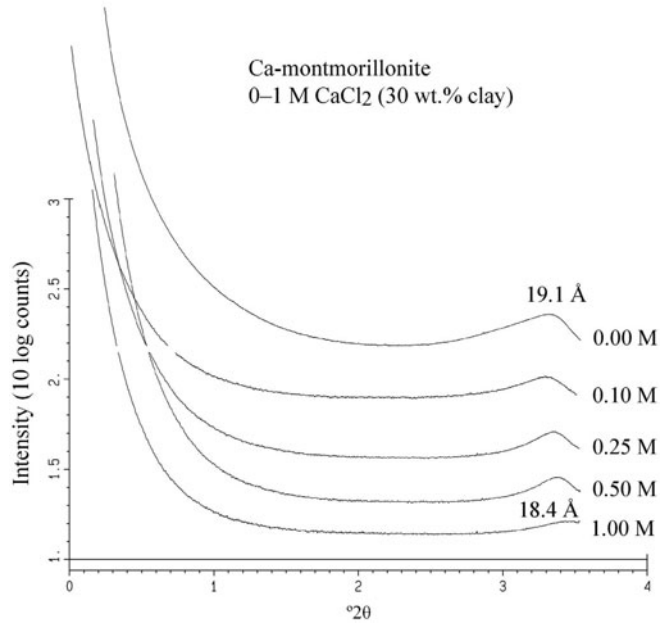

Figure 3. Small-angle X-ray scattering profiles of Ca-montmorillonite in 0−1 M $CaCl_2$ (30 wt.% clay; λ = 1.099 Å).

The frozen sample showed diffraction spots from coarse ice crystals in the two-dimensional XRD patterns as two or three grainy rings in the peripheral parts of the XRD pattern (depending on the sample−detector distance). The integrated intensity of the hydrohalite phase (normalized to the montmorillonite 4.48 Å reflection) showed that the amount of hydrohalite formed was fairly proportional to the salt content in the starting solution (Figure 8d). No systematic difference was noted in the basal spacing comparing the −50 and −100ºC data (Figure 8a).

In the time-resolved freezing data of Na-montmorillonite in 3 M NaCl from 20 to −50ºC (Figure 5a), the basal spacing increased somewhat during the lowering of the temperature (~0.2 Å; 15.9−16.1 Å; Figure 5b). After the ice and hydrohalite had begun to form, the basal spacing decreased again. During thawing the reverse trend was observed, and so all processes were totally reversible (Figure 5c).

Ca-montmorillonite in 0−3 M $CaCl_2$ solution: WAXS at 20, −50, −100, and −130ºC

At 20ºC the basal distance decreased at greater electrolyte strengths, from 19.4 (0 M) to 18.8 Å (1 M) and above 1.5 M to ~15.5 Å (Figure 6). At −50 and −100ºC the opposite was noted; the basal spacing increased as the electrolyte strength increased. At 0 M, W2 (15.8 Å) was identified, and at 0.25 M both W2 and W3, and at higher concentrations only W3 (at ~18 Å; Figure 6) were recorded. As in the Na-case, no systematic difference was seen in the basal spacing for the −50 and −100ºC data (Figure 8c).

Time-resolved freezing data of Ca-montmorillonite in 3 M $CaCl_2$ from 20 to −130ºC (Figure 7) indicated that the basal spacing increased in a stepwise manner as the temperature decreased, and at the point of the ice formation the basal spacing decreased somewhat. The ice formed at ~−75ºC in the kinetic experiment (the nitrogen flow temperature was documented when ice first appeared on the XRD patterns). Minor amounts of antarcticite were observed in different experiments (Figure 8d).

MX-80 bulk bentonite in deionized and natural Äspö ground water: WAXS at 20 and −50ºC

The Äspö water is rather rich in calcium (4510 mg/L; 0.11 M), sodium (3420 mg/L; 0.15 M), and chloride (13500 mg/L; 0.38 M; Table 1). At 20ºC the MX-80 in deionized water showed a combination of a free swelling WX phase and a discrete 001 W3 reflection (19.4 Å; Figure 9a), which was an effect of the composition of the interlayer cations (Na^+, Ca^{2+}), as well as the presence of soluble accessory minerals such as gypsum in the bentonite. In the Äspö groundwater, the MX-80 montmorillonite was a W3 phase with distinct 001 (19.1 Å) and 002 reflections. This was expected from the large Ca content in the Äspö water causing the montmorillonite to ion exchange from Na to Ca-montmorillonite. At −50ºC the MX-80 montmorillonite in the frozen Äspö water showed mixed W2 and W3 phases (a broad reflection with a maximum at 17 Å), while in the sample in deionized water only W2 (15.8 Å) was observed. The W2-W3 mixed state may be interpreted as a Hendricks-Teller reflection indicating mixed-layering of mont-

https://doi.org/10.1346/CCMN.2013.0610412 Published online by Cambridge University Press

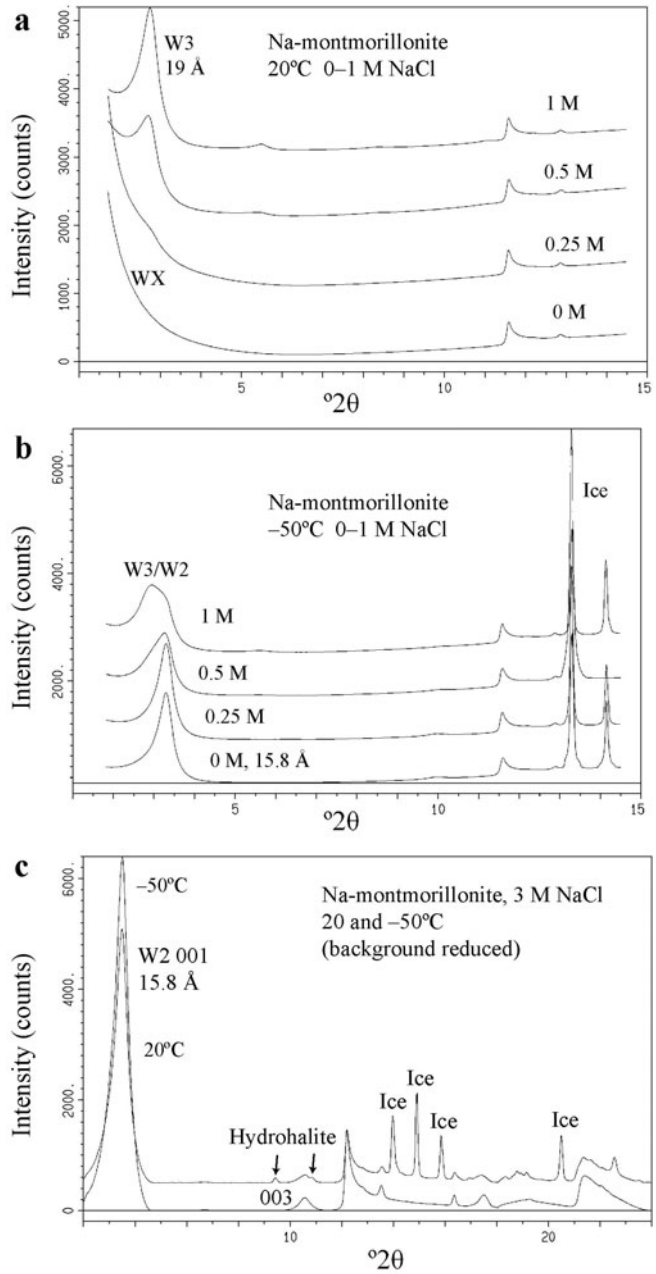

Figure 4. Na-montmorillonite pastes (30 wt.% solids) with 0−1 M electrolyte solution at (a) +20 and (b) −50ºC (λ = 0.9084 Å), and (c) Na-montmorillonite pastes at 3 M electrolyte solution at +20 and −50ºC (λ = 0.955 Å).

morillonite with non-uniform hydration. Within each clay tactoid, heterogeneity such as differences in local cation composition (Na^+, Ca^{2+}) or layer charge may be present. This may cause differences in the hydration properties. Such a suggestion was supported by Slade *et al*. (1991) who concluded that the hydration of montmorillonite in NaCl solutions is a function of the smectite layer charge. That assertion could have been further investigated here by determining the rationality of the basal reflections but was deemed to be outside the scope of the present work. The average basal spacing was consequently greater in the deionized water compared to the Äspö groundwater at 20ºC, while the opposite was true at −50ºC.

Wide-angle X-ray scattering in water at high temperatures (20, 60, and 90ºC)

The Ca-montmorillonite sample (30 wt.% in water) was heated and cooled consecutively in the following sequence: 20 → 60 → 20 → 90 → 20ºC in a sealed

https://doi.org/10.1346/CCMN.2013.0610412 Published online by Cambridge University Press

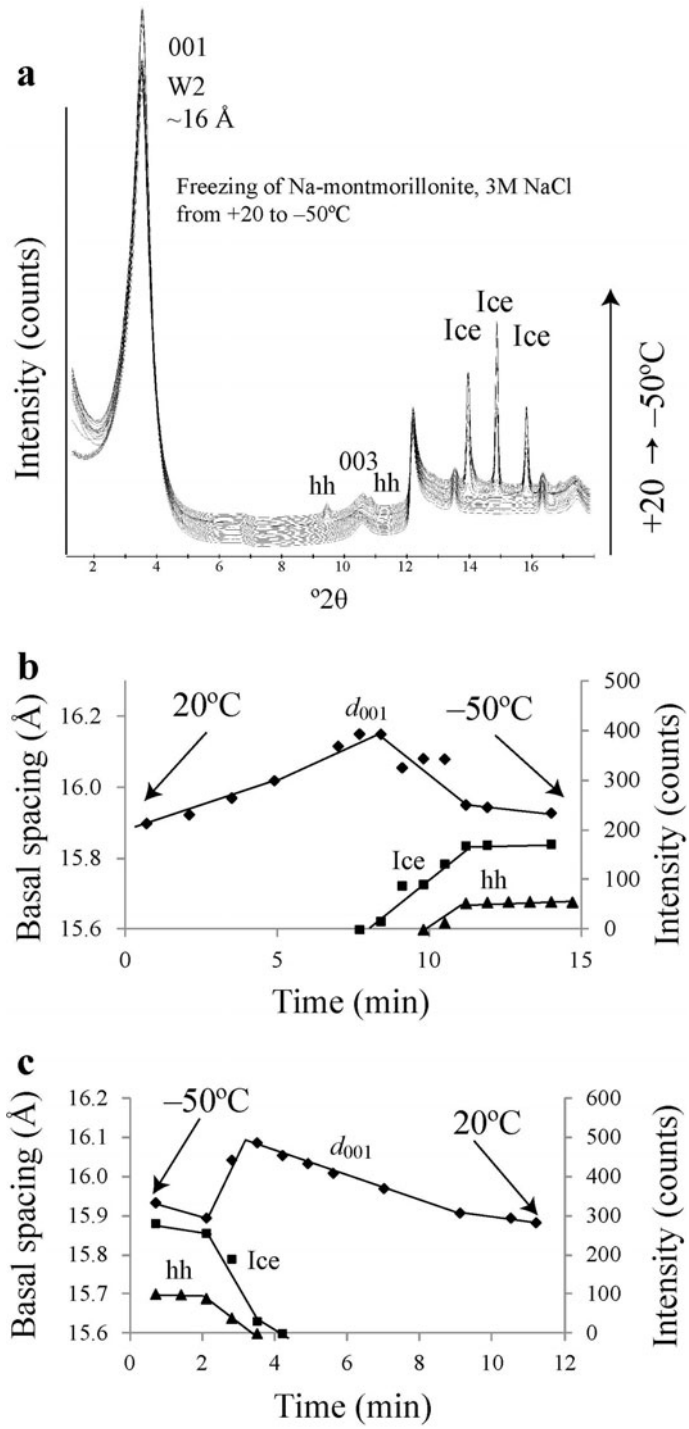

Figure 5. (a,b) Freezing of Na-montmorillonite (30 wt.%) in 3 M NaCl from +20 to −50ºC resolved in time, and (c) thawing from −50 to 20ºC (λ = 0.955 Å). Hh: hydrohalite.

capillary. When the temperature was increased from 20 to 60ºC the basal spacing decreased continuously from 19.9 to 19.5 Å (0.010 Å/K) (Figure 10a). After cooling to 20ºC the basal spacing returned to the original 19.9 Å (Figure 10b). Heating from 20 to 90ºC caused the basal spacing to decrease to 19.4 Å (0.008 Å/K). Final cooling of the sample from 90 to 20ºC increased the basal spacing to 19.7 Å, which was somewhat smaller than the initial one (19.9 Å; Figure 10c).

https://doi.org/10.1346/CCMN.2013.0610412 Published online by Cambridge University Press

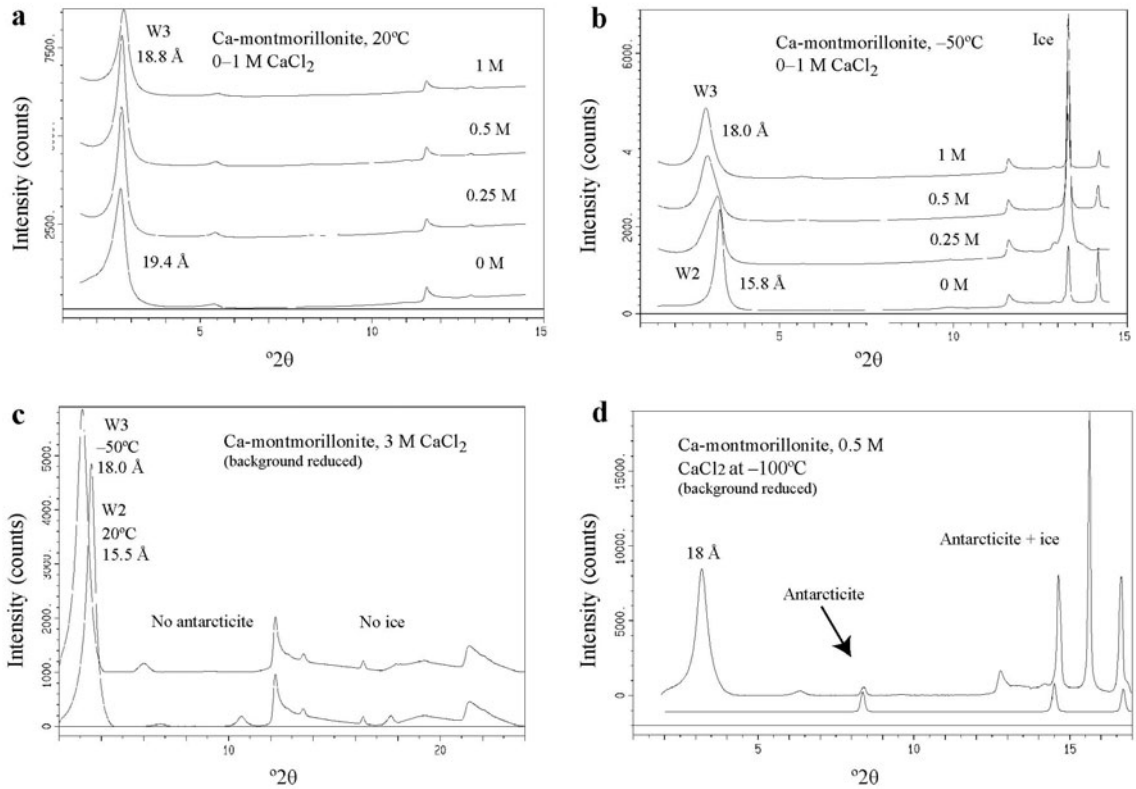

Figure 6. Ca-montmorillonite pastes with 0−1 M electrolyte solution at (a) +20 and (b) −50ºC (λ = 0.908 Å), (c) 3 M electrolyte solution at +20 and −50ºC (λ = 0.955 Å), and (d) at 0.5 M also showing antarcticite together with a calculated antarcticite profile (λ = 0.994 Å).

Free and restricted swelling in montmorillonite

At 20ºC, the basal spacing of Ca-montmorillonite was restricted to ~19 Å corresponding to three water layers (Figure 3). This is normally regarded as the upper limit of swelling in montmorillonite with divalent ions in pure water, and has been referred to as crystalline swelling (Norrish, 1954). In the case of Na-montmorillonite, the basal spacing increased with increasing water content beyond the limits of crystalline swelling. In pure water the Na-montmorillonite basal spacing depended on the solid:liquid ratio (Figure 1). At 90% water content a basal spacing of ~280 Å was identified. The swelling beyond four layers of water (~21 Å) was recognized by Norrish (1954) and was referred to as the second region of swelling, corresponding to ~30−90 wt.% water. In even more disperse systems, a thixotropic gel is formed, which at further dilution turns into a sol, corresponding to the third region of swelling (Norrish, 1954).

The clay used in the experiment was W1 (Na-montmorillonite equilibrated to ~50% relative humidity) and had a basal spacing of ~12.5 Å before the water was added. Based on the following assumptions, the basal spacings of the expanded Na-montmorillonite were proposed to be related to low montmorillonite/water ratios (basal spacing >40 Å; based on the 20−40 Å "forbidden gap" (Norrish, 1954; Fukushima, 1984)): (1) all Na-montmorillonite layers expand equally; (2) the volume of the expanded montmorillonite is equal to the sum of the original montmorillonite plus the volume of added water (both montmorillonite and water densities are regarded constant); (3) the molar mass of the W1 montmorillonite used was 806 g/mol, based on the molar mass for the anhydrous Wyoming montmorillonite, M = 734.28 g mol^{-1}, calculated from the unit-cell formula $(Al_{3.1}Fe_{0.4}Mg_{0.5})(Si_{7.9}Al_{0.1})O_{20}(OH)_4$ and Na ions in the interlayer positions (Karnland *et al*., 2006, p. 116), and assuming ~4 water molecules per unit cell in a W1 montmorillonite (Strunz, 1970); (4) all water is positioned in the interlayer space; and (5) the montmorillonite cell dimensions are a = 5.17, b = 8.94 Å, β = 99.9º (monoclinic; Roberts *et al*. 1974). Using c = 9.5 Å, this corresponds to a density of 2.78 g/cm^3 for anhydrous montmorillonite. The calculations ignore the turbostraticity of montmorillonite as it has little or no effect on the unit-cell volume.

One W1 montmorillonite unit cell has a mass of $806/6.022 \times 10^{23}$ g = 133.8×10^{-23} g. At 10 wt.% montmorillonite, the mass of water is $(90/10) \times 133.8 \times 10^{-23}$ g = 1204.6×10^{-23} g. This

https://doi.org/10.1346/CCMN.2013.0610412 Published online by Cambridge University Press

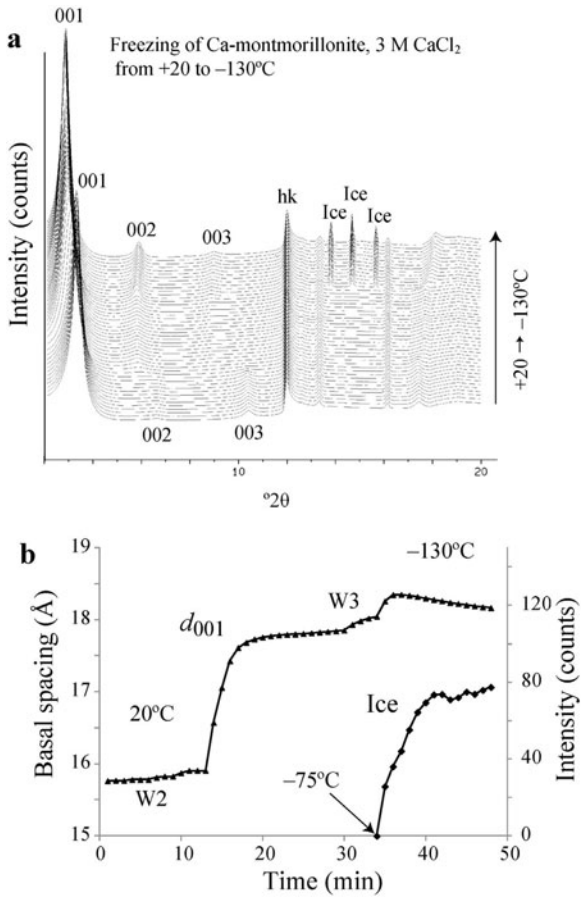

Figure 7. Freezing of Ca-montmorillonite (30 wt.%) in 3 M $CaCl_2$ from +20 to −130ºC resolved in time. (a) Consecutively recorded XRD patterns and (b) basal spacing and ice intensity as a function of time (temperature). λ = 0.955 Å.

corresponds to the volume 1204.6×10^{-23} cm^3 = 12046 $Å^3$. Using the *a* and *b* unit-cell dimensions of the montmorillonite, the water volume would add the following height to the *c* dimension: 12046 $Å^3/(5.17 \times 8.94 \times (\sin\ 99.9º)\ Å^2)$ = 12046/45.6 = 264 Å. The expanded montmorillonite basal spacing becomes: 264 + 12.5 = 276.3 Å. The assumptions used are probably more correct with greater water/clay ratios. As the calculated basal spacing is a sum, the result is insensitive to errors in the W1 basal spacing; this is in contrast to other methods where the calculated basal spacing is a product of the W1 spacing and other factors.

One of the most difficult parameters to measure accurately is the number of water molecules per unit cell of W1 montmorillonite. If one assumes 4.5 water molecules per W1 unit cell, for example, the molar mass becomes 734.3 + 4.5 × 18 = 815.3 g/mol, with a corresponding recalculated basal spacing of 12.5 Å + (12185 $Å^3$/45.58 $Å^2$) = 12.5 Å + 267.3 Å = 279.8 Å. This value matches well the observed value of ~280 Å (Figure 1), based on visual observation of the diffraction maximum. If the assumption that some of the water is outside of the interlayer region is incorrect, the amount of water that is not in the interlayer should be removed and, hence, the calculated basal spacing would decrease. However, due to the extremely platy nature of montmorillonite, the surface of the edges is much smaller compared to the interlayer surface.

Using these same assumptions, the basal spacings for other montmorillonite/water ratios were calculated. For 30, 50, 70, and 80 wt.% Na-montmorillonite, the calculated and observed values were 81 Å and ~88 Å (Figure 1), 42 Å and ~45 Å, 25 Å and ~34 Å, and 20 Å and ~19 Å, respectively.

Several uncertainties exist both in the calculations above and in the determination of the true basal spacing of the montmorillonite at such low angles. Determining the exact position of the reflection was difficult as the background scattering was very high and also because the scattering factor and the Debye-Waller temperature factor decrease almost exponentially with increasing 2θ angle. This brings the maximum of the very broad reflections toward somewhat lower angles (greater *d* spacing). This compensation was also ignored by Fukushima (1984), and so any differences in the results are from other factors. To determine the peak maximum properly, one should compensate for this effect. One may conclude that the swelling of Na-montmorillonite at greater water content (basal spacing >40 Å) is fairly well described as the sum of the volume of the dry clay and the volume of the water. At basal spacings between 20 and 40 Å, Norrish (1954) found a "forbidden gap" with water which was distributed heterogeneously, and hence this region is not well described by these calculations. Actually, in the case of 70 wt.%, both a 34 Å and a minor very broad ~20 Å reflection were seen, which suits well a theoretical average of 25 Å. At very low water content the assumptions are probably less valid, and also the mixing of water and clay becomes more problematic. The basal spacings found in the present study were somewhat greater compared to previously published data (*e.g.* Norrish, 1954; Fukushima, 1984). In the present studies, however, the montmorillonite used was a salt-free, homoionic Na-montmorillonite purified by dialysis which was not the case in the studies of Norrish or Fukushima. Norrish (1954) used an oriented clay film of Wyoming montmorillonite that was saturated consecutively with various electrolyte solutions prior to X-ray measurement. Fukushima (1984) used a natural Na-dominated montmorillonite (Kunipia F) with interlayer cations of 87% Na^+, 10% Ca^{2+}, and 3% K^+. The presence of small amounts of divalent ions in the interlayer has great impact on the swelling of the montmorillonite at large water contents (Birgersson *et al.* 2009), so differences are expected. Wyoming montmorillonites with smaller water contents have been investigated extensively using XRD and modeled to evaluate heterogeneity in hydration (*e.g.* Ferrage *et al.* 2005b) and porosity (*e.g.* Holmboe *et al.* 2012).

https://doi.org/10.1346/CCMN.2013.0610412 Published online by Cambridge University Press

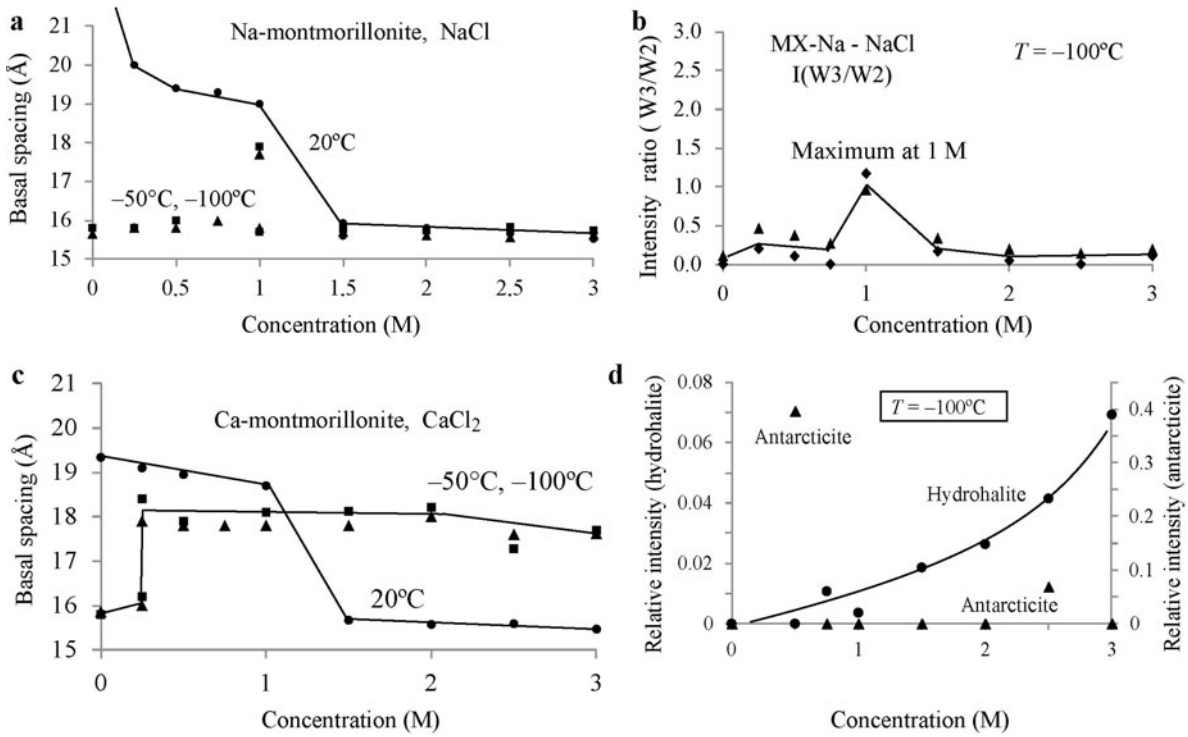

Figure 8. The electrolyte concentrations shown correspond to initial salt concentration at 20ºC; during freezing, the concentration increased, however. (a) Basal spacing of Na-montmorillonite as a function of electrolyte concentration at +20ºC, −50ºC (squares), and −100ºC (triangles). (b) Evolution of the W3 and W2 phases in Na-montmorillonite as a function of electrolyte concentration at −100ºC [presented as intensity ratios *I*(W3 002/W2 003) (diamonds) and *I*(W3 001/W2 001) (triangles)]. (c) Basal spacing of Ca-montmorillonite as a function of electrolyte concentration at +20ºC, –50ºC (squares), and –100ºC (triangles). (d) Hydrohalite and antarcticite formation as a function of electrolyte concentration at –100ºC (presented as relative intensity normalized to the 4.48 Å montmorillonite *hk* reflection).

The swelling of montmorillonite is a balance of attractive and repulsive forces, and the Na-montmorillonite swells until the water activity is leveled out within the system. The situation is different in the Ca-montmorillonite, which has restricted swelling. The osmotic force can be described by the van′t Hoff equation:

$$\Pi = CRT \quad (1)$$

where C is the molar concentration of species in solution, R is the gas constant, and T is the temperature. As C is two times larger in Na-montmorillonite than in Ca-montmorillonite, the osmotic force also becomes two times greater. A semi-quantitative model based on the attractive and anisotropic ion-ion correlation force was also described by Kjellander *et al*. (1988) based on theoretical statistical-mechanical calculations (excluding hydration effects) and experiments measuring the surface force between muscovite crystals in $CaCl_2$ solution using a spring device. This ion-ion correlation effect causing an attractive force was used to explain the restricted swelling of montmorillonite with divalent ions. The balance between attractive and repulsive forces must be very delicate as a small change in the net negative charge localization of the smectite silicate structure is enough to inhibit the free swelling, which is the case in Na-saponite and in some of the Na-beidellites as well (Suquet *et al*. 1975). Interestingly, both Li-saponite and Li-beidellites were found to swell freely (Suquet *et al*. 1975).

Combined salt and temperature dependence on the montmorillonite hydration

In samples free of salt, dominated by water, as in this case, and in the presence of air, the water-vapor pressure $p(H_2O)$ will first follow the boiling curve of pure liquid water upon cooling; later, after freezing, it follows the sublimation curve of pure ice, at least as a first approximation. At 20ºC, $p(H_2O)$ is 24 Torr and at −50ºC it is 0.03 Torr (*CRC Handbook*, 1972), the system thus becomes much drier at lower temperatures, which explains the transition from free-swelling to W2 for the sodium system and from W3 to W2 for the calcium system (Figure 8).

When salt is added to the water, the water potential decreases and the boiling-point curve of water is displaced to lower pressures, which at the same time causes a freezing-point depression and a boiling-point elevation. The lowering of the boiling-point curve becomes more pronounced with the addition of more

https://doi.org/10.1346/CCMN.2013.0610412 Published online by Cambridge University Press

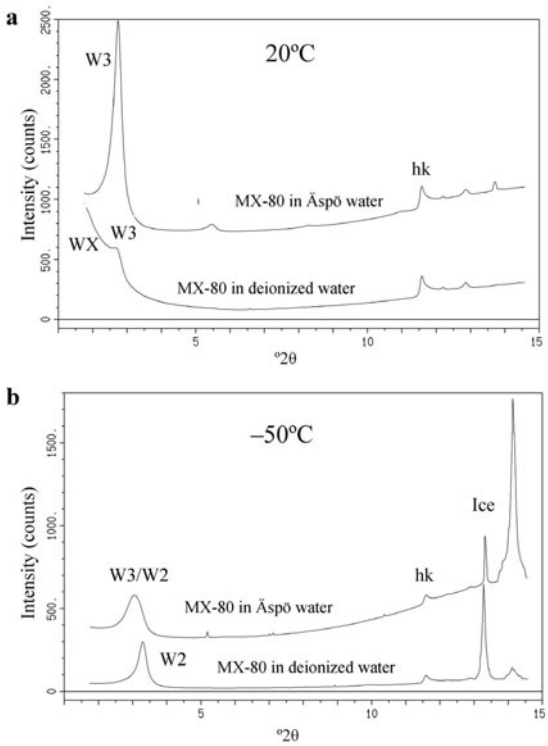

Figure 9. MX-80 bentonite pastes (30 wt.% solids) with deionized water and natural Äspö groundwater at (a) +20 and (b) −50ºC (λ = 0.9084 Å).

salt. This phenomenon is described in most introductory textbooks in chemistry. After ice has formed, the vapor pressure follows the sublimation curve of pure ice, irrespective of the initial salt concentration and the presence of other phases, as long as the ice consists of pure water (Schnewberger *et al*. 1978; Morillon *et al*. 1999). This is usually not emphasized in textbooks and implies that the water partial pressure is constant, *e.g.* −50ºC in all samples containing ice, independent of starting electrolyte strength. In the following discussion, the ice formed is assumed to be chemically pure, and the ice is assumed to be in chemical equilibrium with the interlayer water at the end of the reaction (this is based on the very small size of the montmorillonite particles in relation to the water diffusivity).

In the Na-montmorillonite-NaCl-H_2O system at −50 and −100ºC, in almost all cases W2 + NaCl·$2H_2O$ (hydrohalite) + ice was observed. The existence of the same hydrate (W2) in all of the sodium-containing samples fits well with the presence of a constant partial pressure of water and the fact that the eutectic point in the binary system NaCl-H_2O is at −21ºC and 5.1 M NaCl (Eagleson, 1993). Below the eutectic temperature, the NaCl-H_2O binary system contains solids only. The montmorillonite hydration was unexpectedly at a maximum with starting concentration of ~1 M at −50 and −100ºC (Figure 8).

In the system Ca-montmorillonite-$CaCl_2$−H_2O at −50ºC, the situation is more complex, *i.e.* W2 is present for 0 and 0.25 M $CaCl_2$, while for greater concentrations (0.75−3.0 M) W3 is observed (Figure 8c). Based on a constant partial pressure of water vapor over pure ice, this suggests that the properties of the Ca-montmorillonite change. The introduction of salt (cation and anion) into the montmorillonite interlayer due to the Gibbs-Donnan effect has recently been discussed rather extensively (Karnland *et al*., 2005; Birgersson and Karnland, 2009; Hedström and Karnland, 2011). The amount of interlayer salt is expected to increase with increasing concentration in the surrounding solution. As the ionic concentration increases in the montmorillonite interlayer during the introduction of salt, the water activity is lowered in the clay mineral. Hence, the balance between the water activity of the montmorillonite and the ice is shifted in such a way that less ice is formed at the expense of greater hydration of the montmorillonite. The eutectic point in the binary system $CaCl_2$-H_2O is at −55ºC and 3.8 M $CaCl_2$ (Eagleson, 1993). The presence of one or two of these phases, in addition to W2/W3, was indicated in the different samples.

Observation of salt intercalation in the montmorillonite interlayer has been made in several systems. Evidence for $CaCl^+$ and $MgCl^+$ complexes being adsorbed by Wyoming montmorillonite was found by

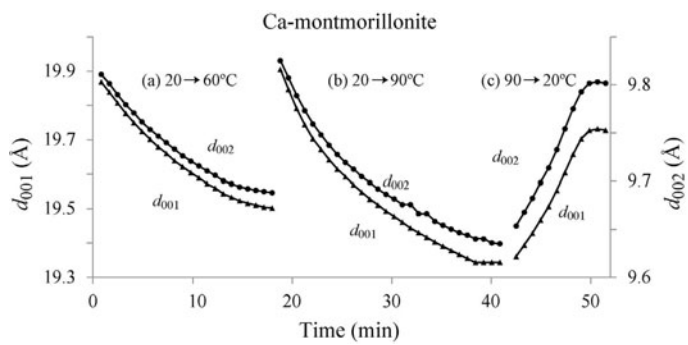

Figure 10. Ca-montmorillonite basal spacing as a function of temperature given as d_{001} (dots) and d_{002} (triangles). Three consecutive series: (a) 20→60ºC, (b) 20→90ºC, and (c) 90 → 20ºC.

https://doi.org/10.1346/CCMN.2013.0610412 Published online by Cambridge University Press

Sposito *et al*. (1983), who investigated the difference between uptake of chloride and perchlorate salts. Ferrage *et al*. (2005a) found support for ion-pair formation in the montmorillonite interlayer by preparing Ca-montmorillonite in deionized and salt water. In XRD measurements, the basal spacing was changed to greater spacings in the sample prepared in salt water, indicating a change in the interlayer composition. Karnland *et al.* (2005) made similar conclusions when comparing experimental swelling pressure data with model calculations of confined Na-montmorillonite in contact with 0−3 M NaCl solutions. The model suggested that the measured swelling pressures could only be explained by introducing Na^+ and Cl^- from the salt solution to the interlayer space of the montmorillonite, hence changing the potential of the interlayer water. The amount of ions was described quantitatively by the Donnan equation. The data (Karnland *et al*. 2005) do not allow the distinction between ion pairs or fully dissociated ions entering the interlayer, though both cations and anions may enter in some form.

In the present study, evidence for salt intercalation was found by observation of changes in dehydration behavior at freezing temperatures (Figure 8). In most cases the Na-montmorillonite-NaCl-ice system formed the salt hydrate hydrohalite upon freezing, while the Ca-montmorillonite–$CaCl_2$–ice system formed only small amounts of the salt hydrate, antarcticite. Instead, the salt and the water occupied the montmorillonite interlayer, which resulted in greater basal spacing.

Temperature changes have previously been observed to affect the hydration of Ca-montmorillonite. For example, in deionized liquid water a partial expansion from 19 to 21 Å was observed as the water cooled (Svensson and Hansen, 2010). In the present study, similar observations were also made in saline systems. Layer expansion occurred during cooling and, to further confirm this behavior, Ca-montmorillonite in liquid water dehydrated with increasing temperature (Figure 10). This temperature-dependent hydration/dehydration is analogous to the observation that the hydration number of Ca^{2+} ions in aqueous $CaCl_2$ increases with decreasing temperature (Zavitsas, 2005). The change in the extent of hydration is compatible with the temperature impact on the Gibbs free energy:

$$\Delta G = \Delta H - T\Delta S \quad (2)$$

Any reaction will occur spontaneously if $\Delta G < 0$, which is a function of the reaction enthalpy (ΔH) and the reaction entropy (ΔS), and depends parametrically on the temperature T. Introducing more water molecules to increase the hydration of Ca corresponds to an exothermic reaction (more bonds are formed, negative enthalpy), though the system becomes increasingly ordered by the larger amount of molecules introduced and the process is thus balanced by the negative change in entropy. As the temperature decreases, the impact from entropy on the Gibbs free energy will also decrease because the entropy term is directly proportional to the temperature.

Freezing of bentonite buffer in engineered safety barriers

Engineering barriers with compacted bentonite as a buffer material are used in several applications such as final repositories of spent nuclear fuel and final storage of radioactive waste from the deconstruction of nuclear power plants. The bentonite buffer may freeze if situated too close to the surface, and the freezing causes a net expansion of the system as ice has a larger molar volume than either bulk or interlayer water. This increase in volume may fracture the surrounding rock because of an increase in pressure. The ice formation also impacts the plasticity of the buffer. At a depth of 500 m, anticipated for final storage of high-level nuclear waste in crystalline rock in Sweden, the freezing of the bentonite buffer is currently not considered a problem. This is based on a minimum temperature of −2ºC during permafrost conditions (SKB, 2006) and a freezing point in compacted bentonite of −4 to −11ºC (MX-80 at 1950−2050 kg/m^3 bulk density; Birgersson *et al.* 2009). However, shafts situated closer to the surface that are backfilled with smectite-rich clay and with other kinds of storage of low- or intermediate-level radioactive waste may freeze. When small amounts of salts are introduced, the extent of ice formation and montmorillonite dehydration is reduced by the additional cations and anions in the montmorillonite interlayer lowering the potential of the interlayer water, and hence retarding the formation of ice. The effect was considerable, especially with calcium salt where the hydrated ions stayed as interlayer ions, contrary to the sodium case where, instead, an external hydrohalite phase formed. This is a positive effect from the safety perspective of the repository. The results also show a general trend of expansion of the montmorillonite with decreasing temperature (before ice formation; especially for Ca ions; explained by the temperature impact of the hydration entropy); this effect of increased montmorillonite hydration would probably increase the swelling pressure in a confined volume of bentonite buffer. A future interesting study would be to measure the swelling pressure of a confined system at buffer densities contacted with various likely electrolyte combinations as a function of realistic temperatures.

ACKNOWLEDGMENTS

Financial support by the Swedish Nuclear Fuel and Waste Management Co (SKB) is gratefully acknowledged. Many thanks to Ola Karnland, Martin Birgersson, and Magnus Hedström at Clay Technology AB, Lund, for stimulating discussions. The authors also thank Carin Österberg and Dennis Ivarsson for practical help at the MAX-lab synchrotron.

REFERENCES

Ahlrichs, J.L. and White, J.L. (1962) Freezing and lyophilizing alters the structure of bentonite gels. *Science, New Series*, **136**, 1116–1118.

Amorim, C.L.G., Lopes, R.T., Barroso, R.C., Queiroz, J.C., Alves, D.B., Perez, C.A., and Schelin H.R. (2007) Effect of clay–water interactions on clay swelling by X-ray diffraction. *Nuclear Instruments and Methods in Physics Research Section A: Accelerators, Spectrometers, Detectors and Associated Equipment*, **580**, 768–770.

Anderson, D.M. and Hoekstra, P. (1965) Migration of interlamellar water during freezing and thawing of Wyoming bentonite. *Soil Science Society of America Journal*, **29**, 498–504.

Birgersson, M. and Karnland, O. (2009) Ion equilibrium between montmorillonite interlayer space and an external solution – consequences for diffusional transport. *Geochimica et Cosmochimica Acta*, **73**, 1908–1923.

Birgersson, M., Karnland, O., and Nilsson, U. (2008) Freezing in saturated bentonite – A thermodynamic approach. *Physics and Chemistry of the Earth*, Parts A/B/C. **33**, Supplement 1, S527–S530.

Birgersson, M., Börgesson, L., Hedström, M., Karnland, O., and Nilsson, U. (2009) Bentonite erosion – final report. Swedish Nuclear Fuel and Waste Management Co – Technical report. SKB TR-09-34, Svensk Kärnbränslehantering AB, Stockholm.

Bradley, W.F., Grim, R.E., and Clark, W.I. (1937) A study of the behavior of montmorillonite upon wetting. *Zeitschrift für Kristallographie*, **97**, 216–222.

Brindley G.W. and Brown, G. (1980) *Crystal Structures of Clay Minerals and their X-ray Identification*. Monograph No. **5**, Mineralogical Society, London.

Cerenius, Y., Ståhl, K., Svensson, L.A., Ursby, T., Oskarsson, Å., Albertsson, J., and Liljas, A. (2000) The crystallography beamline I711 at MAX II. *Journal of Synchrotron Radiation*, **7**, 203–208.

CRC Handbook (1972) *Handbook of Chemistry and Physics*, 53rd edition. CRC Press, Division of the Chemical Rubber Co., Boca Raton, Florida, USA

Eagleson, M. (1993) *Concise Encyclopedia of Chemistry*. Walter de Gruyter, Berlin.

Ferrage, E., Tournassat, C., Rinnert, E., Charlet, L., and Lanson, B. (2005a) Experimental evidence for Ca-chloride ion pairs in the interlayer of montmorillonite. An XRD profile modelling approach. *Clays and Clay Minerals*, **53**, 348–360.

Ferrage, E., Lanson B., Sakharov, B.A., and Drits, V.A. (2005b) Investigation of smectite hydration properties by modeling experimental X-ray diffraction patterns. Part I. Montmorillonite hydration properties. *American Mineralogist*, **90**, 1358–1374.

Fukushima, Y. (1984) X-ray diffraction study of aqueous montmorillonite emulsions. *Clays and Clay Minerals*, **32**, 320–326.

Hedström, M. and Karnland, O. (2011) Donnan equilibrium in Na-montmorillonite from a molecular dynamics perspective. *Geochimica et Cosmochimica Acta*, **77**, 266–274.

Holmboe, M., Wold, S., and Jonsson, M. (2012) Porosity investigation of compacted bentonite using XRD profile modeling. *Journal of Contaminant Hydrology*, **128**, 19–32.

Huang, T.C., Toraya, H., Blanton, T.N., and Wu, Y. (1993) X-ray-powder diffraction analysis of silver behenate. A possible low-angle diffraction standard. *Journal of Applied Crystallography*, **26**, 180–184.

Karnland O., Muurinen A., and Karlsson F. (2005) Bentonite swelling pressure in NaCl solutions. Pp. 241–256 in: *Experimentally Determined Data and Model Calculations. Advances in Understanding Engineered Clay Barriers* (E.E. Alonso and A. Ledesma, editors). Taylor & Francis Group, London.

Karnland, O., Olsson, S., and Nilsson, U. (2006) Mineralogy and sealing properties of various bentonites and smectite-rich clay material. SKB Technical Report, TR-06-30, Svensk Kärnbränslehantering AB, Stockholm.

Kjellander, R., Marčelja, S., Pashley, R.M., and Quirk, J.P. (1988) Double-layer ion correlation forces restrict calcium-clay swelling. *Journal of Physical Chemistry*, **92**, 6489–6492.

Light, B., Brandt, R.E., and Warren, S.G. (2009) Hydrohalite in cold sea ice: Laboratory observations of single crystals, surface accumulations, and migration rates under a temperature gradient, with application to "Snowball Earth". *Journal of Geophysical Research*, **114**, C07018.

Low, P.F., Anderson, M., and Hoekstra, P. (1968) Some thermodynamic relationships for solids at or below the freezing point. 1. Freezing point depression and heat capacity. *Water Resources Research*, **4**, 379–394.

Mammen, C.B., Ursby, T., Cerenius, Y., Thunnissen, M., Als-Nielsen, J., Larsen, S., and Liljas, A. (2002) Design of a 5-station macromolecular crystallography beamline at MAX-lab. *Acta Physica Polonica A*, **101**, 595.

Mammen, C.B., Ursby, T., Cerenius, Y., Thunnissen, M., and Als-Nielsen,J. (2004) Bent diamond crystals and multilayer based optics at the new 5-station protein crystallography beamline 'Cassiopeia' at MAX-lab. *AIP Conference Proceedings*, 705, 808–811.

Morillon, V., Debeaufort, F., Jose, J., Tharrault, J.F, Capelle,M., Blond, G., and Voilley, A. (1999) Water vapour pressure above saturated salt solutions at low temperatures. *Fluid Phase Equilibria*, **155**, 297–309.

Norrish, K. (1954) The swelling of montmorillonite. *Discussions of the Faraday Society*, **18**, 120–134.

Norrish, K. and Rausell-Colom, J. (1962) Effect of freezing on the swelling of clay minerals. *Clay Minerals Bulletin*, **5**, 9–16.

Roberts, W.L., Rapp, G.R., and Weber, J. (1974) *Encyclopedia of Minerals.* Van Nostrand Reinhold Company, New York.

Schnewberger, R., Voilley, A., and Weisser, H. (1978) Activity of water in frozen systems. *International Journal of Refrigeration* **1**, 201–206.

Segad, M., Jönsson, B., Åkesson, T., and Cabane B. (2010) Ca/Na montmorillonite: Structure, forces and swelling properties. *Langmuir*, **26**, 5782–5790.

Slade, P.G., Quirk, J.P., and Norrish, K. (1991) Crystalline swelling of smectite samples in concentrated NaCl solutions in relation to layer charge. *Clays and Clay Minerals*, **39**, 234–238.

Sposito, G., Holtzclaw, K.M., Charlet, L., Jouany, C., and Page, A.L. (1983) Sodium-calcium and sodium-magnesium exchange on Wyoming bentonite in perchlorate and chloride ionic media. *Soil Science Society of America Journal*, **47**, 51–56.

SKB (2006) *Climate and climate-related issues for the safety assessment SR-Can*. SKB TR-06-23, Svensk Kärnbränslehantering AB, Stockholm.

Suquet, H., De La Calle, C., and Pezerat, H. (1975) Swelling and structural organization of saponite. *Clays and Clay Minerals*, **23**, 1–9.

Svensson, P.D. and Hansen, S. (2010) Freezing and thawing of montmorillonite – a time-resolved synchrotron X-ray diffraction study. *Applied Clay Science*, **49**, 127–134.

Strunz, H. (1970) *Mineralogische Tabellen*, 5th edition. Geest & Portig Akademische Verlagsgesellschaft, Leipzig, Germany.

Tambach, T.J., Hensen, E.J.M., and Smit, B. (2004) Molecular simulations of swelling clay minerals. *Journal of Physical*

https://doi.org/10.1346/CCMN.2013.0610412 Published online by Cambridge University Press

Chemistry B, **108**, 7586–7596.
Torii, T. and Ossaka, J. (1965) Antarcticite: a new mineral, calcium chloride hexahydrate, dicovered in Antarctica. *Science* **149**, 975–977.
Zavitsas, A.A. (2005) Aqueous solutions of calcium ions: Hydration numbers and the effect of temperature. *The Journal of Physical Chemistry B*, **109**, 20636–20640.

(*Received 6 November 2012; revised 23 July 2013; Ms. 724; AE: R. Dohrmann*)